*American Mineralogist, Volume 62, pages 710–720, 1977*

# Stereochemical systematics of ordered $C2/c$ silicate pyroxenes

PAUL H. RIBBE AND ARTHUR R. PRUNIER, JR.

*Department of Geological Sciences*
*Virginia Polytechnic Institute and State University*
*Blacksburg, Virginia 24061*

**Abstract**

Multiple regression analysis has been used to determine the relationships among the formal charges and Shannon-Prewitt radii of the non-tetrahedral $M1$ and $M2$ cations in thirteen $C2/c$ (or $C2$) pyroxenes and their lattice parameters, their mean $M$–O and Si–O bond lengths, and their O3–O3–O3 chain angles. Crystal-structure data from three groups of silicate pyroxenes (both natural and synthetic) were used in the regression analyses: Li pyroxenes with trivalent Al, Fe, and Sc in the $M1$ sites, Na pyroxenes with trivalent Al, Cr, Fe, Sc, and In in the $M1$ sites, and Ca pyroxenes with divalent Ni, Mg, Co, Fe, and Mn in the $M1$ sites.

Using only first-order linear regression equations in terms of the radii of the $M1$ and $M2$ cations ($r_{M1}$ and $r_{M2}$) and the charge $q$ on the $M2$ cation, it was found statistically that more than 98.5 percent of the variation in the $a$ cell dimension can be attributed to the variation in $r_{M1}$ alone, and 97.5 percent in $b$ can be attributed to variations in both $r_{M1}$ and $r_{M2}$. The parameters $c \sin \beta$ and unit-cell volume require a third term, $q$, to produce the most highly significant regression equations: $c \sin \beta$ has a standard error of estimate (SEE) of 0.011 A and volume 2.2 A$^3$. The mean $M1$–O distance is linearly related only to $r_{M1}$ (SEE = 0.007 A) and the mean $M2$–O distance to both $r_{M2}$ and $r_{M1}$ (SEE = 0.013 A) or, more significantly, to $r_{M1}$, $r_{M2}$, *and* $q$ (SEE = 0.009 A). Both the mean Si–O bridge bond lengths (range: 1.624–1.688 A) and the grand mean Si–O distances (range: 1.618 to 1.644 A) may be estimated to better than 0.004 A, and the tetrahedral chain angle O3–O3–O3 (range: from 163.8° in the O-rotated chain of johannsenite to 189.5° in the S-rotated chain of spodumene) to better than 2.6°, using a regression equation in three terms.

Because it has been shown that the effective radius of the $M2$ cation (or the $\langle M2\text{–O}\rangle$ distance) is not independent of the size of the $M1$ cation, it is possible to rationalize the distinctly non-linear curves of volume *vs.* $(r_{M1})^3$ for the isostructural series NaAl–NaCr–NaFe–NaTi–NaSc–NaIn, and LiAl–LiFe–LiSc, as well as the series CaNi–CaMg–CaCo–CaFe–CaMn, which has an opposite curvature from the pyroxenes with monovalent $M2$ cations.

## Introduction

Crystal-chemical studies of the pyroxenes are numerous, but we, in the course of a classroom exercise, have produced yet another which pertains to the ordered clinopyroxenes of $C2/c$ (or $C2$) symmetry, specifically those with Ca, Na, or Li in the $M2$ site and Si in the tetrahedral site(s). At present count thirteen such structures have been refined, some of them more than once. Where there was a choice, we selected data from the more recent study (see Table 1). The preliminary account of our work (Ribbe and Prunier, 1976) has been subjected to considerable revision.

Relationships between cell dimensions and chemical composition have been extensively investigated for naturally occurring orthopyroxenes (Smith *et al.*, 1969) and synthetic orthopyroxenes (Turnock *et al.*, 1973). Turnock *et al.* have also calculated trend surface equations for the clinopyroxenes in the diopside–hedenbergite–ferrosilite–enstatite (CaMg–CaFe–FeFe–MgMg) quadrilateral based on 62 synthetic one-phase samples, many of which must be considered metastable because of their crystallization within the two-phase region or in the stability field of orthopyroxenes. Third-order trend surfaces gave the best fit for $a$, $b$, $c$, and $\beta$, while a fourth-order equation was required for volume. The authors (p. 57) "emphasize that the data are not directly appli-

Table 1. Lattice parameters, mean bond lengths, interatomic angles, and effective ionic radii for 13 ordered clinopyroxenes.

| Formula | (Ref.) | $a$ | $b$ | $c$ | $\beta$ | Volume | <$M1$-O> | <$M2$-O> | <Si-O> | <Si-O>$_{br}$ | O3-O3-O3 | $r_{M1}$ | $r_{M2}$ |
|---|---|---|---|---|---|---|---|---|---|---|---|---|---|
| $LiAlSi_2O_6$ | (1) | 9.449Å | 8.386Å | 5.215Å | 110.1° | 388.1Å$^3$ | 1.919Å | 2.211Å | 1.618Å | 1.624Å | 189.5° | 0.530Å | 0.740Å |
| $LiFeSi_2O_6$ | (1) | 9.666 | 8.669 | 5.294 | 110.2 | 416.4 | 2.031 | 2.249 | 1.620 | 1.626 | 180.0 | 0.652* | 0.742* |
| $LiScSi_2O_6$ | (2) | 9.803 | 8.958 | 5.352 | 110.3 | 440.8 | 2.107 | 2.289 | 1.624 | 1.630 | 175.6 | 0.745 | 0.740 |
| $NaAlSi_2O_6$ | (3) | 9.423 | 8.564 | 5.223 | 107.6 | 401.8 | 1.929 | 2.469 | 1.625 | 1.634 | 174.6 | 0.530 | 1.160 |
| $NaCrSi_2O_6$ | (3) | 9.579 | 8.722 | 5.267 | 107.4 | 420.0 | 1.998 | 2.489 | 1.624 | 1.643 | 172.1 | 0.615 | 1.160 |
| $NaFeSi_2O_6$ | (1) | 9.658 | 8.795 | 5.294 | 107.4 | 429.1 | 2.025 | 2.518 | 1.628 | 1.642 | 174.0 | 0.645 | 1.160 |
| $NaScSi_2O_6$ | (4) | 9.844 | 9.044 | 5.354 | 107.2 | 455.3 | 2.102 | 2.564 | 1.632 | 1.653 | 173.6 | 0.745 | 1.160 |
| $NaInSi_2O_6$ | (5) | 9.902 | 9.131 | 5.359 | 107.2 | 462.9 | 2.141 | 2.568 | 1.632 | 1.652 | 170.8 | 0.800 | 1.160 |
| $CaNiSi_2O_6$ | (6) | 9.737 | 8.899 | 5.231 | 105.9 | 435.9 | 2.072 | 2.494 | 1.634 | 1.673 | 165.1 | 0.690 | 1.120 |
| $CaMgSi_2O_6$ | (1) | 9.746 | 8.899 | 5.251 | 105.8** | 438.2 | 2.077 | 2.498 | 1.635 | 1.676 | 166.4 | 0.720 | 1.120 |
| $CaCoSi_2O_6$ | (6) | 9.797 | 8.954 | 5.243 | 105.4 | 443.4 | 2.102 | 2.506 | 1.634 | 1.674 | 164.8 | 0.745 | 1.120 |
| $CaFeSi_2O_6$ | (3) | 9.845 | 9.024 | 5.245 | 104.7 | 450.6 | 2.130 | 2.511 | 1.635 | 1.676 | 164.5 | 0.780 | 1.120 |
| $CaMnSi_2O_6$ | (7) | 9.978 | 9.156 | 5.293 | 105.5 | 466.0 | 2.173 | 2.530 | 1.644 | 1.688 | 163.8 | 0.830 | 1.120 |

(1) Clark *et al.* (1969), (2) Hawthorne and Grundy (1976), (3) Cameron *et al.* (1973), (4) Hawthorne and Grundy (1973), (5) Hawthorne and Grundy (1974), (6) Schlenker *et al.* (1977), (7) Freed and Peacor (1967).

* All radii from Shannon and Prewitt (1969, revised 1970) for the ordered clinopyroxenes; these values are adjusted to account for the slightly $Fe^{2+}$-rich formula reported by Clark *et al.* (1969, p. 33, Table 4) for LiFe pyroxene.

** The β angle of 105.6° reported by Clark *et al.* (1969) disagrees with every other value reported for diopside. See Nolan and Edgar (1963), Finger and Ohashi (1976), Warner and Luth (1974), Rutstein and Yund (1969) and the comments by Schlenker (1976) on whose recommendation we decided to use 105.8° in our regression analysis. Note also that the 105.6° β angle for diopside is the only anomalous value in Figure 5 (p. 597) of Cameron *et al.* (1973).

cable to natural pyroxenes, since other elements in the latter may affect unit-cell parameters." They do not attempt to relate lattice parameters to site occupancy. Their paper is an excellent review of earlier work on pyroxenes in the quadrilateral (*e.g.*, Rutstein and Yund, 1969). Nolan (1969) determined unit-cell dimensions and refractive indices for synthetic clinopyroxenes in the system diopside–hedenbergite–acmite ($CaMg$–$CaFe^{2+}$–$NaFe^{3+}$), and found nearly linear variations of $a$, $b$, $c$, and $\beta$ with composition between end members. Variations of refractive indices were not quite as simple, but a ternary plot contoured for $b$ and $\alpha$ refractive index *vs.* composition proved to be a reasonable determinative method for natural alkali pyroxenes, provided the substitution of Al, and $Fe^{3+}$ for Si in the tetrahedral chain and Ti (in octahedral coordination?) was very limited.

The early classic work on the crystal-chemical characterization of clinopyroxenes is that of Clark *et al.* (1969), who discussed the structures of eight of the "end-member" ordered pyroxenes (LiAl, LiFe, NaAl, NaCr, NaFe, NaIn, CaMg, and CaMn) that presently concern us. Since then the crystal structures of five other pyroxenes have been published: CaFe (Cameron *et al.*, 1973), CaNi and CaCo (Schlenker *et al.*, 1977; Ghose and Wan, 1975), and NaSc and LiSc (Hawthorne and Grundy, 1973 and 1977 respectively). New refinements of NaAl (Cameron *et al.*, 1973) and NaIn (Hawthorne and Grundy, 1974) pyroxenes complete our data set. A plethora of structural studies of pyroxenes at high temperatures has recently appeared; among them are those involving ordered $C2/c$ end-members (Cameron *et al.*, 1973; Ohashi and Burnham, 1973; Finger and Ohashi, 1976) and others which invert to $C2/c$ symmetry at elevated temperatures (*e.g.*, Brown *et al.*, 1972; Smyth and Burnham, 1972; Smyth, 1974). Our investigation, however, is restricted to the structures of ordered phases at room temperature whose symmetry is $C2/c$ or $C2$.

The $C2$ structures are the $LiM^{3+}$ pyroxenes which differ from the $C2/c$ $NaM^{3+}$ and $CaM^{2+}$ structures in two respects: (1) the Li ion (radius $r$ = 0.74 A) is six-coordinated, whereas Na ($r$ = 1.16 A) and Ca ($r$ = 1.12 A) are considered to be eight-coordinated, and (2) the smaller Li causes very slight structural distortions which produce two symmetrically non-equivalent $M1$ sites and two symmetrically non-equivalent $M2$ sites in the octahedral layer and two Si sites in the single tetrahedral chain. However, these distortions are so slight and the deviation from $C2/c$

symmetry so small that "even the temperature factors for the [LiAl and LiFe] spodumenes refined in $C2/c$ are entirely comparable to those found in other ordered clinopyroxenes" (Clark *et al.*, 1969, p. 42). We have therefore taken the average structures of the Li$M^{3+}$ pyroxenes and examined them together with the other ordered $C2/c$ pyroxenes.

## Results of regression analyses

There is merit in knowing exactly what the relationships are between the lattice parameters, the bond lengths and angles, and the effective ionic radii of atoms occupying the coordination polyhedra in so important a group as the ordered $C2/c$ silicate pyroxenes, and we propose to explore them. Other investigators have suggested some of these: (1) Clark *et al.* (1968) mentioned that "the *b* cell-dimension of the Na and Ca clinopyroxenes is found empirically to be a linear function of the average $M1$–O distance." (2) Prewitt *et al.* (1972) and Hawthorne and Grundy (1974) plotted lattice parameters as a function of the radius of the $M1$ cation, $r_{M1}$, or $(r_{M1})^3$ for the Na$M^{3+}$ pyroxenes, and the latter authors have in press a comparison of the geometric parameters of the Li$M^{3+}$ and Na$M^{3+}$ pyroxenes which were discussed earlier by Brown (1971). (3) Papike *et al.* (1973, p. 264) have elaborated on the topologies of pyroxene structures, noting "that the ionic charge of the cations occupying $M(2)$ and $M(1)$ cation sites should also be taken into consideration" in the obvious relation "between the mean ionic radius of the $M(2)$ and $M(1)$ cations . . . and the tetrahedral chain angle O(3)–O(3)–O(3)" in $C2/c$ pyroxenes (*cf.* their Fig. 4, p. 260). (4) Ghose and Wan (1975) recognized four distinct groups of $C2/c$ pyroxenes (Li$M^{3+}Si_2O_6$, Na$M^{3+}Si_2O_6$, Ca$M^{2+}Si_2O_6$ and Ca$M^{3+}AlSiO_6$) "in all of which the average $M2$–O distances increase linearly with an increase in the average $M1$–O distance. In each series, an increase in the $M1$-octahedron results in a simultaneous increase in the kinking of the tetrahedral chain and a slight increase in the $T$–O (brg.) and O3–O3′ (tetrahedral edge) distances."

By contrast with previous investigators, our initial approach was to use the standard techniques of multiple linear regression analysis (Dixon, 1973) to systematize relationships between the Shannon and Prewitt (1969, 1970) effective ionic radii of the $M1$ and $M2$ cations and the unit-cell parameters, the mean $M1$–O, $M2$–O and Si–O distances, and the O3–O3–O3 chain angle. Later it was found necessary to introduce a term to account for the charge $q$ on the $M2$ cation.

### *The ⟨M1–O⟩ and ⟨M2–O⟩ distances*

As expected, the mean $M1$–O distances, ⟨$M1$–O⟩, are very highly correlated (coefficient of determination $R^2 = 0.993$) with the radii of the $M1$ cations, $r_{M1}$ (Fig. 1 and Table 2). But ⟨$M2$–O⟩ distances correlate less well with $r_{M2}$, and a glance at Figure 1 suggests a strong interdependence on $r_{M1}$ as well. For a given $M2$ cation, ⟨$M2$–O⟩ increases with size of either the trivalent cations or the divalent cations in $M1$ (see Ghose and Wan, 1975). Multiple regression produces a significantly improved correlation (Fig. 2) where the regression coefficient for $r_{M1}$ is more than half as great as that for $r_{M2}$ (Table 2). On the graph of calculated *vs.* observed ⟨$M2$–O⟩ values there are still discrete populations for the Na and Ca pyroxenes. This may be due to inadequate estimates of the effective radii of Na and/or Ca, or, as will appear later, the need to introduce a third term into the regression equation.

The relationship between ⟨$M2$–O⟩ and the radius of the $M1$ cation is probably due to the fact that the $M2$ polyhedron shares three edges with octahedra of the $M1$ chain. A similar effect was noted in the Ca–garnets, in which the mean Ca–O distance is observed to increase with increasing radius of the trivalent cations (Al, Cr, Fe) in octahedra which share

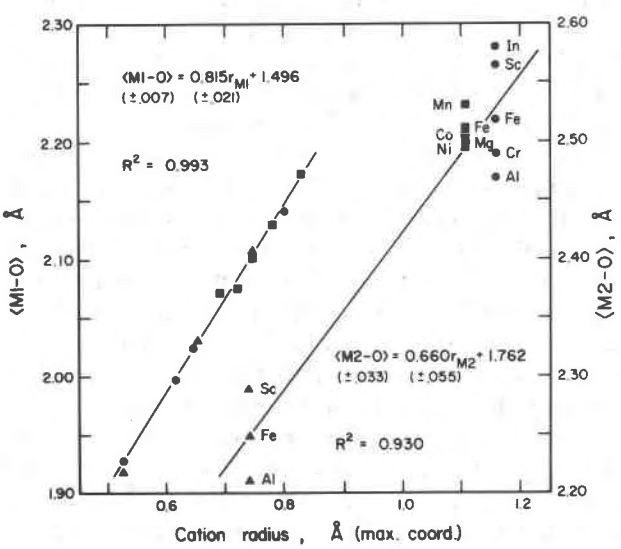


Fig. 1. Plots of the radii of the $M1$ cations *vs.* the mean of the $M1$–O bond lengths (left ordinate) and the radii of the $M2$ cations *vs.* the mean of the $M2$–O bond lengths (right ordinate) for 13 ordered clinopyroxenes. Regression equations (with estimated standard errors in brackets) are given for the lines shown. $R^2$ is the coefficient of determination. Li-pyroxenes are designated by triangles, Na-pyroxenes by circles, and Ca-pyroxenes by squares.

Table 2. Regression coefficients, intercepts, and error and significance statistics for selected lattice parameters and bond distances and interatomic angles in 13 ordered clinopyroxenes. (Degrees of freedom: 11 for equations in one independent variable, 10 for those in two, and 9 for those in three variables. To calculate $|t|$, divide the regression coefficient by its standard error.)

| Parameter | Regression coefficient(s) $r_{M1}$ (std. error) | | $r_{M2}$ (std. error) | | $q$ (std. error) | | Intercept | Range of residuals (std. error of est.) | | Multiple correl. coef. (coef. of determ. = $R^2$) | | F value* |
|---|---|---|---|---|---|---|---|---|---|---|---|---|
| $a$ | 1.728 | (0.064) | | | | | 8.525 | 0.059 | (0.021) | 0.993 | (0.985) | 728 |
| $a\sin\beta$ | 1.729 | (0.087) | 0.357 | (0.043) | 0.090 | (0.017) | 7.583 | 0.060 | (0.025) | 0.995 | (0.991) | 316 |
| $b$ | 2.160 | (0.123) | 0.265 | (0.067) | | | 7.083 | 0.110 | (0.039) | 0.987 | (0.975) | 193 |
| | 2.275 | (0.120) | 0.295 | (0.060) | -0.049 | (0.023) | 7.039 | 0.085 | (0.034) | 0.992 | (0.983) | 174 |
| $c\sin\beta$ | 0.545 | (0.039) | 0.198 | (0.019) | -0.035 | (0.007) | 4.499 | 0.026 | (0.011) | 0.989 | (0.977) | 129 |
| Volume | 235.32 | (7.91) | 30.79 | (3.94) | -5.92 | (1.53) | 247.06 | 6.48 | (2.25) | 0.996 | (0.993) | 420 |
| <*M1*-O> | 0.815 | (0.021) | | | | | 1.496 | 0.023 | (0.007) | 0.997 | (0.993) | 1553 |
| <*M2*-O> | 0.321 | (0.041) | 0.614 | (0.022) | | | 1.587 | 0.040 | (0.013) | 0.995 | (0.992) | 506 |
| | 0.370 | (0.033) | 0.627 | (0.017) | -0.021 | (0.006) | 1.568 | 0.027 | (0.009) | 0.998 | (0.995) | 652 |
| $\langle Si\text{-}O\rangle_{br}$ | 0.062 | (0.014) | 0.040 | (0.007) | 0.029 | (0.003) | 1.529 | 0.009 | (0.004) | 0.988 | (0.976) | 124 |
| <Si-O> | 0.036 | (0.013) | 0.016 | (0.006) | 0.006 | (0.002) | 1.580 | 0.007 | (0.004) | 0.912 | (0.832) | 15 |
| O3-O3-O3 | -26.19 | (9.01) | -19.17 | (4.49) | -6.61 | (1.74) | 219.33 | 8.27 | (2.56) | 0.954 | (0.910) | 30 |

* See Dixon (1973) for definition and usage.

edges with the $CaO_8$ polyhedron (Novak and Gibbs, 1971; see Fig. 2 in Higgins and Ribbe, 1977).

### *The a cell dimension*

Statistically, the most significant correlation between the *a* cell dimension and cation radius is represented by the equation $a = 1.728r_{M1} + 8.525$, which for the 13 ordered structures has a standard error of estimate of 0.021 A (Fig. 3). The *a* dimension is obviously a measure of the thickness of the octahedral layer, and although $a\sin\beta$ might have been considered a better measure, regression statistics do not bear this out (Table 2). What is interesting to note is that the addition of $r_{M2}$ to the regression analysis does not improve the estimate of *a*, as though the size of the *M*2 polyhedron does not affect the thickness of the octahedral layer. (The coefficient of determination of a linear regression between $r_{M2}$ and *a* is only 0.06.) This is explained by the fact that these irregular polyhedra, containing large Na or Ca cations, are free to expand laterally into the rift zone between octahedral bands and are flattened normal to (100), as shown in Figure 3 of Clark *et al.* (1969, p. 38). Thus, it is to be expected that the size of the *M*2 cation influences *b*, which is a measure of the width of the octahedral band, and *c*, which is a measure of its unit length.

### *The b cell dimension*

Clark *et al.* (1968) recognized the relation between *b* and ⟨*M*1–O⟩, and indeed the equation $b = 2.29r_{M1} + 7.27$ produces a standard error of estimate of 0.060 A for the 13 pyroxenes (Fig. 3). But this is reduced to 0.039 A when the $r_{M2}$ term is added (Table 2). Although the regression coefficient for this term is only one-eighth the magnitude of that for $r_{M1}$, its partial correlation coefficient is 0.78, and it significantly improves the coefficient of determination from 0.935 to 0.975 (*cf.* Figs. 3 and 4).

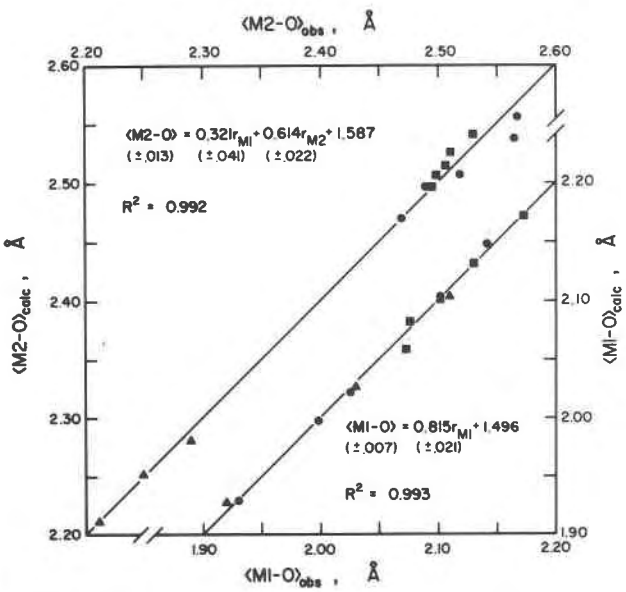


Fig. 2. Plots of the observed *vs.* calculated mean *M*1–O (right ordinate, lower abcissa) and mean *M*2–O distances (left ordinate, upper abcissa). Symbols as in Fig. 1; observed values are listed in Table 1.

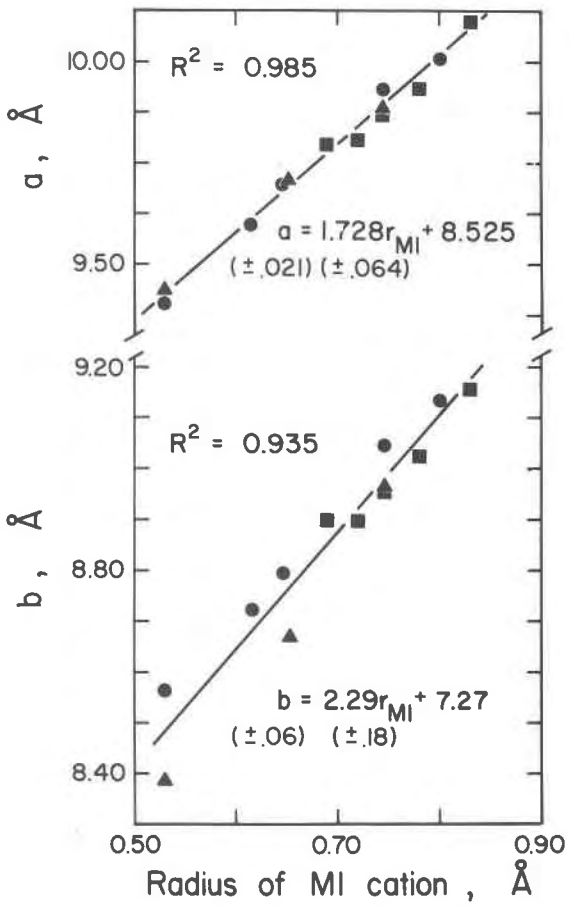


Fig. 3. Plots of the $a$ and $b$ cell dimensions *vs.* the radii of the cations in the $M1$ sites. Symbols as in Fig. 1.

*The c cell dimension and β*

When the $c$ dimensions are plotted against $r_{M1}$, those of the Li and Na pyroxenes fall on a straight line, but the Ca pyroxenes are a distinct population with barely a semblance of order (Fig. 5). A regression equation in terms of both $r_{M1}$ and $r_{M2}$ shows no improvement in predicted values over that in terms of $r_{M1}$ for the $c$ dimension.

Li pyroxenes have a $\beta$ angle of 110.2 ± 0.1° ($\beta$ increasing with $r_{M1}$) and Na pyroxenes have $\beta$ = 107.3 ± 0.3°, ($\beta$ decreasing with $r_{M1}$), but $\beta$ values for Ca pyroxenes are scattered around a mean value of 105.5° (Fig. 5). A regression equation for $\beta$ in terms of $r_{M1}$ and $r_{M2}$ is of no greater value in predicting $\beta$ than knowing the atomic species in $M2$ and guessing $\beta$ to be equal to the mean value for that cation.

By contrast it is most surprising to observe in Figure 5 that three distinctly ordered populations with nearly parallel trends emerge when $c\sin\beta$ is plotted *vs.* $r_{M1}$. Although the Shannon-Prewitt radii for 8-coordinated Na and Ca are very nearly equal ($r_{Na}$ = 1.16 A, $r_{Ca}$ = 1.12 A), the equation $c\sin\beta = 0.463\, r_{M1} + 0.176 r_{M2} + 4.531$ gives a standard error of estimate of 0.019 A and $R^2 = 0.922$. Values of $c\sin\beta$ calculated with this equation are plotted in Figure 6 at the ends of the vertical lines opposite the symbols. Careful examination of these data show that there are still distinct Li, Na, and Ca populations, and that the calculated $c\sin\beta$ values for the Ca pyroxenes lie systematically above the 45° line and those for the Na pyroxenes below it. This same phenomenon was observed for ⟨$M2$–O⟩ in Figure 2 and to lesser degree for $b$ in Figure 4.

In order to compensate for this discrepancy, a third term was added to the regression analysis and tested for all parameters reported in this study. That term is $q$, the formal charge on the $M2$ cation: when $q$ is specified for $M2$, a like term is implied for $M1$, *i.e.*, either $q_{M2} = 2$ and $q_{M1} = 2$ or $q_{M2} = 1$ and $q_{M1} = 3$. As stated earlier, the $q$ term may in part account for inadequate estimates of the effective radii of Na and Ca in 8-fold coordination, and of course a three-parameter equation is expected to give a better fit than a two-parameter regression equation. There are statistical tests to ascertain whether the addition of an independent variable is significant. The Biomedical Computer Programs (Dixon, 1973) use $F$ ratios and the more familiar $|t|$ tests, among others. For example, when $q$ is added to the equation in $r_{M1}$ and $r_{M2}$ for ⟨$M2$–O⟩ (illustrated in Fig. 2), the $F$ value in-

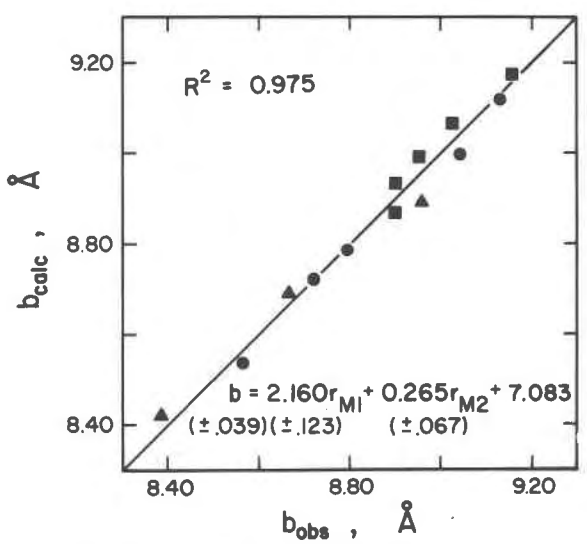


Fig. 4. Plot of the observed *vs.* calculated $b$ cell dimensions using an equation in $r_{M1}$ and $r_{M2}$ from Table 2. Symbols as in Fig. 1.

creases from 506 to 652, the standard error of estimate decreases from 0.013 A to 0.009 A, and with 9 degrees of freedom $|t| = -3.20$ for the $q$ term, indicating an extremely high degree of significance. For the $b$ cell-edge, the significance of the addition of the $q$ term is less clear because $F$ decreases, but $|t| = -2.1$ with 9 degrees of freedom, suggesting that it is not possible at the 95 percent confidence level to reject the hypothesis that the $q$ term is significant (Draper and Smith, 1966, p. 20). The regression data for $\langle M2\text{–O}\rangle$ and $b$ are given in Table 2.

From Figure 6 it is obvious that an equation in $r_{M1}$, $r_{M2}$ and $q$ (Table 2) gives better estimates of $c\sin\beta$ than one in $r_{M1}$ and $r_{M2}$: the standard error of estimate is improved from 0.019 to 0.011 A with an increase in the $F$ ratio from 59 to 128. The computed $|t|$ value for the $q$ term is $-4.65$, and with 9 degrees of freedom it is not possible at the 99.9 percent confidence level to reject the $q$ term.

The fact that $c\sin\beta$ is linearly related to $r_{M1}$ and $c$ and $\beta$ separately are not, indicates that some of the expansion in the pyroxene cell caused by increased size of cations in the octahedral layer is taken up by slight [001] displacements of the tetrahedral chains above and below the octahedral layer, producing

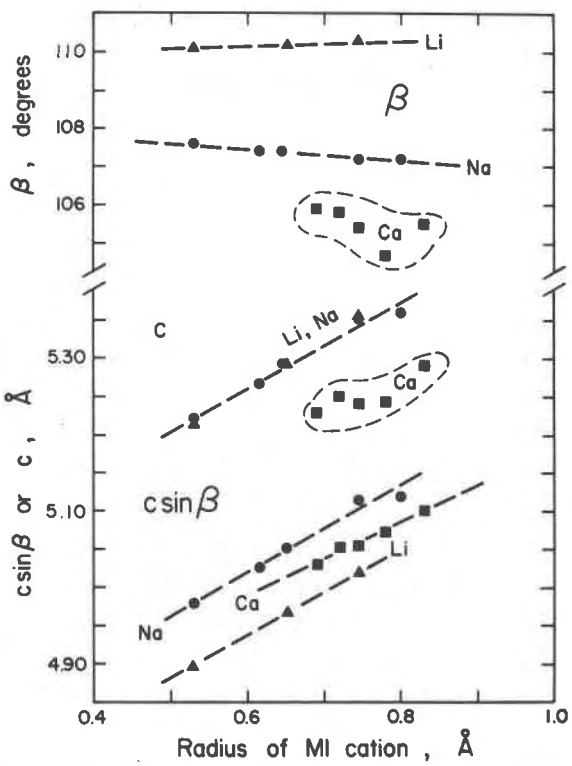


Fig. 5. Plots of $\beta$, $c$, and $c\sin\beta$ *vs.* the radii of the $M1$ cations.

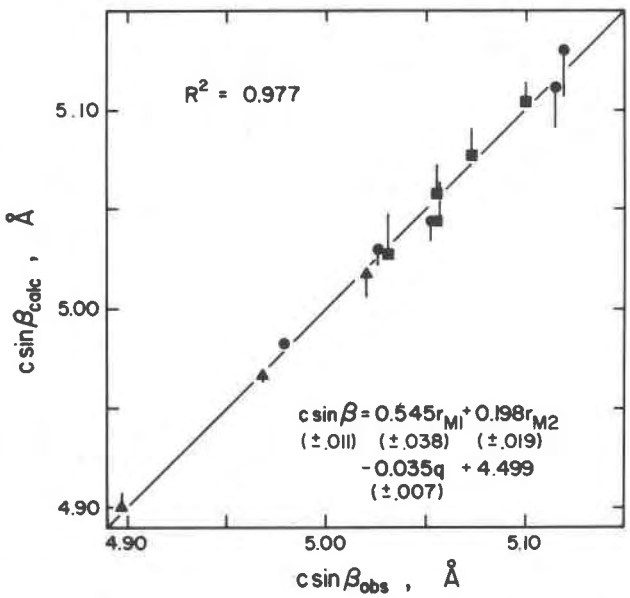


Fig. 6. Plot of observed *vs.* calculated values of $c\sin\beta$. The symbols represent values calculated using the equation in $r_{M1}$, $r_{M2}$, and $q$ (Table 2), whereas the tails of the vertical lines represent values calculated using an equation in $r_{M1}$ and $r_{M2}$ only. Symbols as in Fig. 1.

concomitant small changes in the $\beta$ angle (*cf.* Papike *et al.*, 1973, p. 265).

### *Volume*

It is interesting to note that the $q$ term carries over into the regression equation for volume ($= a \times b \times c\sin\beta$), as indicated by the following self-explanatory data:

$$\text{Vol} = 221.3r_{M1} + 27.1r_{M2} + 252.2$$

(Std. error of estimate, 3.5 A$^3$; $R^2 = 0.981$; $F = 260$)

$$\text{Vol} = 235.3r_{M1} + 30.8r_{M2} - 5.9q + 247.1$$

(Std. error of estimate, 2.2 A$^3$; $R^2 = 0.993$; $F = 420$)

In the latter equation a $|t|$ test indicates that at the 99.5 percent confidence level the $q$ term cannot be rejected.

### *The tetrahedral chain angle, O3–O3–O3*

The $(SiO_3)_\infty$ chain in pyroxenes extends parallel to $c$, and adjacent tetrahedra are related by a $c$ glide (Fig. 7). The chain is nearly straight so that the $c$ cell dimension is slightly less than four times the radius of oxygen: $c \sim 5.2$ to 5.3 A $< 4 \times 1.36$ A. The crenulation of the chain is expressed in terms of the O3–O3–O3 angle, which varies from 189.5° for the S-rotated chain in LiAl pyroxene to 180° for the

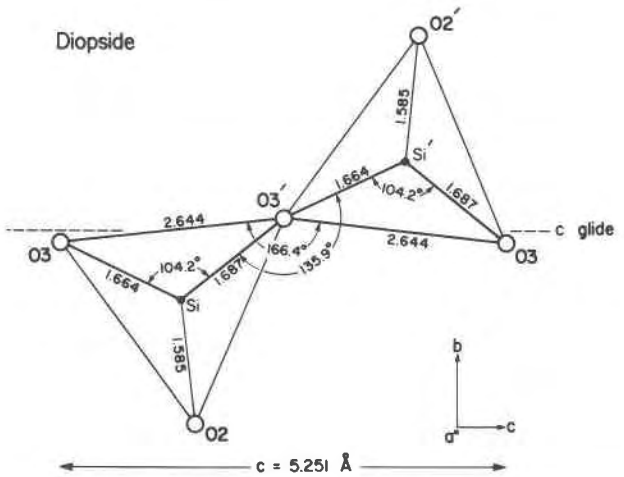


Fig. 7. A schematic drawing of two corner-sharing [$SiO_4$] tetrahedra in the [$SiO_3$]$^{\infty}$ chain of diopside (data from Clark *et al.*, 1969).

straight chain in LiFe pyroxene to 163.8° for the O-rotated chain in CaMn pyroxene.

In the regression analysis of the O3–O3–O3 angle, a remarkable improvement in predicted values is obtained with the addition of the $q$ term to the regression equation in $r_{M1}$ and $r_{M2}$ (Fig. 8). Perhaps it is not immediately obvious why the O3–O3–O3 angle should be related to *any* of these parameters, so the interested reader is referred to the discussion of Papike *et al.* (1973, p. 264–267) for topologic details. But we would comment further that the O3 atom is the bridging oxygen between adjacent tetrahedral sites and also is bonded to either one 6-coordinated $M2$ cation (in the case of $Li^+$ pyroxenes) or two 8-coordinated $M2$ cations (in the case of $Na^+$ and $Ca^{++}$ pyroxenes). Intuitively, then, the charge on the $M2$ cation, the $M2$–O3 distance(s) and the coordination number of O3 all may be expected to affect the O3 position and thus the O3–O3–O3 angle. Clark *et al.* (1969, p. 35–42) hint at this in their discussion of bonding in the ordered clinopyroxenes. It is impossible to miss the implications of the following tabulation, which shows positive correlations between ⟨Si–O3⟩ and the mean of the sums of the formal Pauling bond strengths $S$ to O3, and negative correlations of ⟨Si–O3⟩ and $S$ with the mean O3–O3–O3 angles.

| | $Li^+$ | $Na^+$ | $Ca^{++}$ |
|---|---|---|---|
| Mean Si–O3 (A) | 1.627 | 1.645 | 1.677 |
| Mean $S$ to O3 | 2.167 | 2.250 | 2.500 |
| Mean O3–O3–O3 (°) | 181.7 | 173.0 | 164.9 |

But what of the relation of the magnitude of the tetrahedral chain angle to $r_{M1}$? As we saw earlier, it is the size of the $M1$ cation that largely controls the $c$ dimension for the pyroxenes with monovalent or divalent cations (Fig. 5), but it is also true that $c$ = 2[O3···O3] × sin ½[O3–O3–O3], where [O3···O3] is the length of the edge of the tetrahedron most nearly parallel to $c$ (Fig. 7). Thus Figure 8 and the regression equation in Table 2 represent a simplistic rationalization of the variation of the O3–O3–O3 angle in terms of the charges and radii of the non-tetrahedral cations.

The O3–O3–O3 angle is correlated with the $\beta$ angle ($\beta$ = 0.23[O3–O3–O3] + 67.76; $R^2$ = 0.80) and the mean of the two Si–O3 bridge bonds ($\langle Si\text{–}O\rangle_{br}$ = 2.1140 − 0.0027[O3–O3–O3]; $R^2$ = 0.80). The former arises from relative displacements of the tetrahedral chains above and below the $M2$ site "which are necessary to accommodate changes in coordination around $M(2)$" (Papike *et al.*, 1973, p. 265). The latter is best understood in the terms detailed in the previous paragraphs, keeping in mind that the bridging oxygen atoms $O_{br}$ in the tetrahedral chain are O3 oxygens. Obviously, the greater the Coulombic interaction of O3 with its non-tetrahedral neighbor(s), the longer will be the Si–O3 bond lengths and the greater will be the O rotation of the tetrahedra.

*The Si–O bond lengths*

We have seen that $\langle Si\text{–}O\rangle_{br}$ is correlated to the O3–O3–O3 angle for reasons discussed above, and

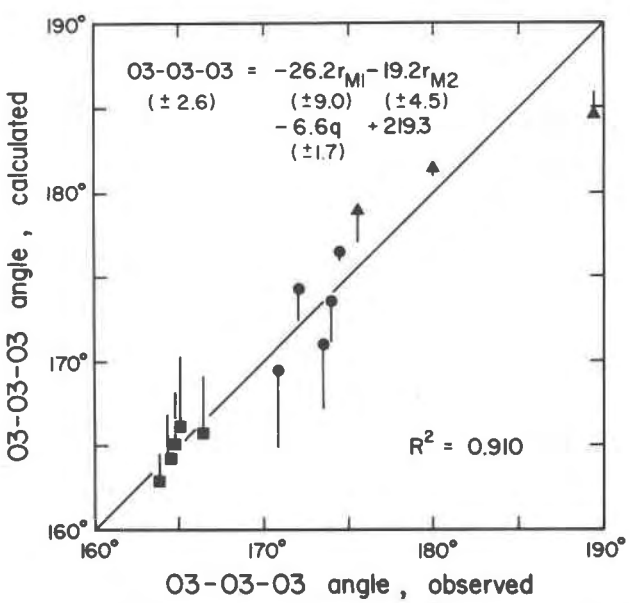


Fig. 8. Plot of observed *vs.* calculated values for the O3–O3–O3 angle. Same symbol convention as in Fig. 6.

thus it comes as no surprise that $\langle Si\text{–}O\rangle_{br}$ is highly correlated to $r_{M1}$, $r_{M2}$, and $q$. In the ordered clinopyroxenes the range of observed mean Si–O3 bonds is 1.624–1.688 A, and as in other regression analyses, there are three distinct populations of data for Li, Na, and Ca pyroxenes when only $r_{M1}$ and $r_{M2}$ are considered in the regression. But when the formal charge on $M2$ is included, the standard error of estimate improves threefold (from 0.013 to 0.004 A) and $R^2$ increases from 0.67 to 0.98. This is well-documented in Figure 9, where the tails of the vertical lines represent calculated values of $\langle Si\text{–}O\rangle_{br}$ using only $r_{M1}$ and $r_{M2}$, and the symbols represent those calculated using $q$ in addition to $r_{M1}$ and $r_{M2}$.

By contrast with the bridging Si–O3 bonds, the non-bridging Si–O1 and Si–O2 bond lengths are on the average longest for Li pyroxenes and shortest for Ca pyroxenes. However, as previously noted for $\langle Si\text{–}O\rangle_{br}$, there is a high correlation of $\langle Si\text{–}O\rangle_{nbr}$ with the Pauling bond strengths $S$ to O1 and O2. The following table summarizes these observations:

| | $Li^+$ | $Na^+$ | $Ca^{++}$ |
|---|---|---|---|
| Mean Si–O1 (A) | 1.635 | 1.631 | 1.607 |
| Mean Si–O2 (A) | 1.593 | 1.592 | 1.588 |
| Mean $\langle Si\text{–}O\rangle_{nbr}$ (A) | 1.614 | 1.612 | 1.595 |
| Mean $S$ to O1 & O2 | 1.834 | 1.813 | 1.754 |

The Si–O2 bonds are relatively constant (see comments by Clark *et al.*, 1969, p. 36), the Si–O1 bonds

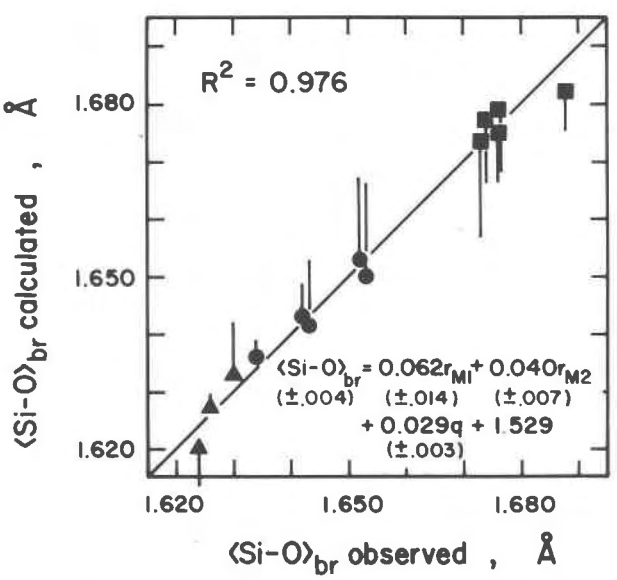


Fig. 9. Plot of observed *vs.* calculated mean Si–O bridge bond-lengths: $\langle Si\text{–}O\rangle_{br}$ = [(Si–O3) + (Si–O3′)] ÷ 2 (*cf.* Fig. 7). Same symbol convention as in Fig. 6.

are highly correlated to $q$ (although *not* to $r_{M1}$ or $r_{M2}$), and the means of the two Si–O3 bridge bonds are highly correlated to $r_{M1}$, $r_{M2}$, and $q$ (Fig. 9). Thus the grand mean Si–O distances may be calculated with the equation

$$\langle Si\text{–}O\rangle = 0.036r_{M1} + 0.016r_{M2} + 0.006q + 1.580,$$

all of whose terms have nearly equal significance, according to $|t|$ tests, and whose standard error of estimate is <0.004 A ($R^2$ = 0.83).

### Evaluation of other data

Figure 10 has been prepared to summarize the lattice parameters of some synthetic $C2/c$ pyroxenes found in the literature. Data for Li pyroxenes are taken from Brown (1971), for NaTi and NaIn pyroxenes from Prewitt *et al.* (1972), and for CaNi and CaCo pyroxenes from Ghose and Wan (1975). Most of these fall within the range of residuals of the calculated values, although many are outside the range of standard errors of estimate as indicated by the parallel diagonal lines.

Twenty-two pyroxenes synthesized by Nolan (1969) in the system CaMg–$CaFe^{2+}$–$NaFe^{3+}$ are represented as dots in Figure 10: end-member data, labeled Di, Hd, and Ac, respectively, are taken from Table 1. The assumption used in our calculations of $a$, $b$, and $c\sin\beta$ is that all of Nolan's pyroxenes are ordered with Na and Ca in $M2$ and the other cations appropriately apportioned in $M1$. The $q$ term is appropriately weighted to give the average charge on $M2$. The extreme consistency of his data with the parameters we used in our regression equations for CaMg (Di), CaFe (Hd), and NaFe (Ac) pyroxenes affirms this assumption, although for this system anything less than ~10 percent disorder would not be detectable within estimated errors.

It is difficult to evaluate the lattice parameters determined by Drysdale (1975) for six Li pyroxenes containing trivalent Al, Cr, Fe, V, Sc, and In, because his estimated standard errors on $a$, $b$, and $c$ are exceptionally large, ranging between 0.01 and 0.03 A. Parameters reported for the LiSc and LiIn pyroxenes are so markedly divergent from values calculated with regression equations (as well as from earlier literature data for LiSc pyroxenes), that we suspect either the stoichiometry of his material or his technique for lattice-parameter determination.

Lattice parameters determined by Abs-Wurmbach and Neuhaus (1976) for 12 compounds in the solid-solution series jadeite ($NaAlSi_2O_6$)–cosmochlore ($NaCrSi_2O_6$) present some difficulty of interpretation,

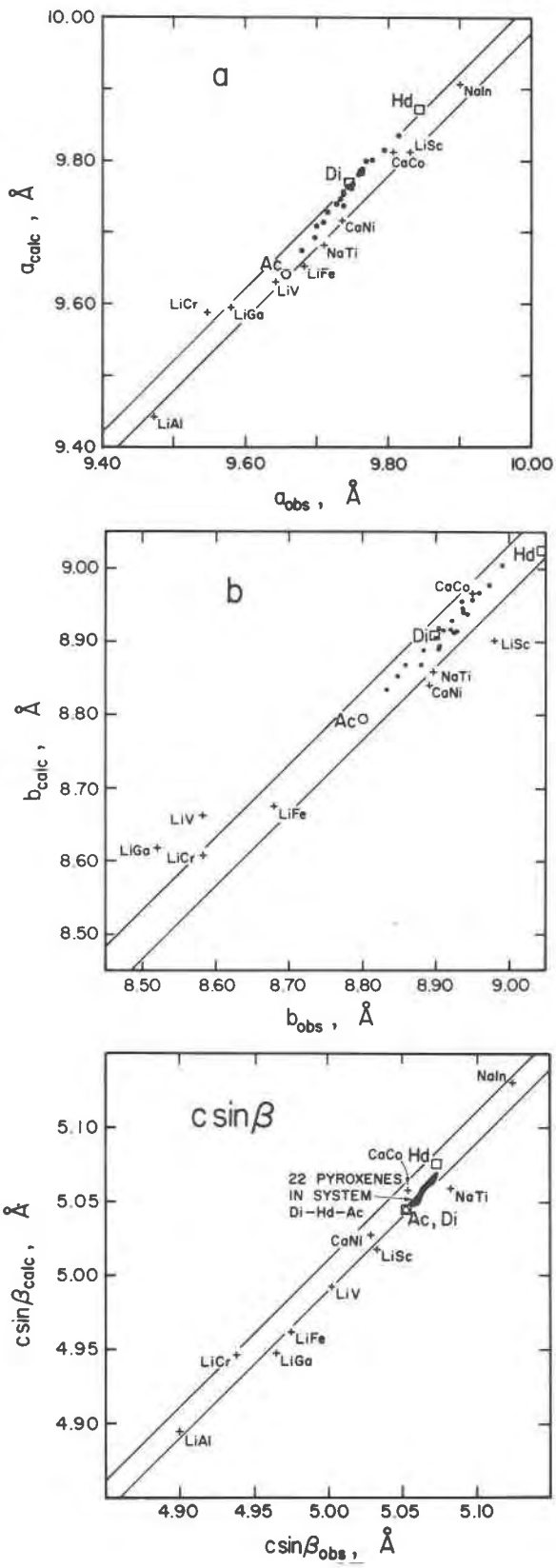


which is not made any simpler by the fact that they omitted $\beta$ angles from their complications and mislabeled the right ordinate of their volume–composition plot. In the synthesis of the NaCr end-member (and perhaps $NaAl_{0.1}Cr_{0.9}$ and $NaAl_{0.2}Cr_{0.8}$), they may have produced a nonstoichiometric or otherwise off-composition product. Their reported volume for NaCr is 417.8 A$^3$, whereas that observed by Cameron *et al.* (1973) on a synthetic material whose structure was determined is 420.0 A$^3$ (Table 1). If the 420.0 A$^3$ value is plotted instead of 417.8 A$^3$, the volume–composition relationship shown by Abs-Wurmbach and Neuhaus (their Fig. 4) becomes linear and no longer requires a third-order equation to fit the data. Furthermore, the 417.8 A$^3$ volume for NaCr falls substantially below the expected value on the Na$M^{3+}$ curve in Figure 11.

Figure 11 is a graph of the relationship between unit-cell volume and the cube of the radius of the $M1$ cation, $(r_{M1})^3$ for the Na, Ca, and Li pyroxenes. Note that the curves for Li$M^{3+}$ and Na$M^{3+}$ are somewhat similar, whereas that for Ca$M^{2+}$ has an opposite curvature. There are so few data points that calculation of a higher than first-order curve for Li is impossible, but second-order curves for Na and Ca pyroxenes have coefficients of determination $R^2 > 0.997$. Additional points for NaTi and NaIn pyroxenes are shown as large open circles. They were taken from Prewitt *et al.* (1972), who expressed concern that the NaIn point in particular did not fit what at that time they assumed should be a straight-line plot of volume *vs.* $(r_{M1})^3$. Our evidence indicates that there is no such simple relationship: volume is a function of *three* parameters, $r_{M1}$, $r_{M2}$, and $q$. Even the "size" of the $M2$ cation is not independent of the effective ionic radius of the cation occupying the edge-sharing $M1$ octahedra. Furthermore, when in our regression analyses we used $(r_{M1})^3$ and $(r_{M2})^3$—with and without $q$—to calculate equations for unit-cell volume, we discovered that these parameters did not account for variations in volume nearly as well as did $r_{M1}$ and $r_{M2}$.

All this simply reemphasizes a fact which has been restated frequently: effective ionic radii, like those

Fig. 10. Plots of observed *vs.* calculated $a$, $b$, and $c\sin\beta$ cell parameters for data selected from the literature. Values for Ac ($NaFeSi_2O_6$), Hd ($CaFeSi_2O_6$), and Di ($CaAlSi_2O_6$) are from Table 1 (open symbols); values for the 22 pyroxenes in the system Ac–Hd–Di (black dots) are from Nolan (1969); values for NaTi and NaIn pyroxenes from Prewitt *et al.* (1972), for Li-pyroxenes from Brown (1971) and for CaCo and CaNi pyroxenes from Ghose and Wan (1975) (crosses). Values for $a$, $b$ and $c\sin\beta$ were calculated from equations in Table 2.

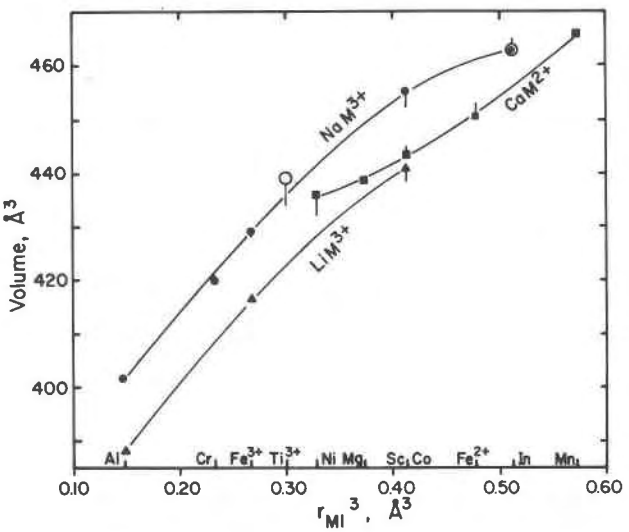


Fig. 11. Plots of the relationships of unit-cell volumes and $(r_{M1})^3$ for the Na$M^{3+}$, Ca$M^{2+}$, and Li$M^{3+}$ pyroxenes. Large open circles are data points from Prewitt *et al.* (1972); tails of vertical lines represent values of volume calculated using the equation in Table 2.

determined by Shannon and Prewitt (1969, 1970), are not "hard" values, even relative to an assumed primary coordination number and oxygen radius. Secondary coordination is important, and these *C*2/*c* ordered pyroxenes demonstrate this especially well for silicon in tetrahedral coordination, because even the mean Si–O bond lengths in these isostructural compounds are strongly correlated to the formal charges and effective sizes of the non-tetrahedral *M*1 and *M*2 cations.

## Summary

The lattice parameters of ordered *C*2/*c* (and *C*2) pyroxenes with Li, Na, or Ca in the *M*2 site may be expressed in terms of the formal valences and effective ionic radii of the non-tetrahedral cations. The *a* cell dimension is a function of $r_{M1}$, *b* of $r_{M1}$ and $r_{M2}$, and $c\sin\beta$ and volume are functions of $r_{M1}$, $r_{M2}$, and *q*, the charge on the *M*2 cation. Multiple regression analyses indicate that the mean *M*1–O distance is best expressed in terms of $r_{M1}$ only, whereas the mean *M*2–O distance, the mean Si–O bridge and grand mean Si–O bond lengths, and the O3–O3–O3 angle require three-parameter equations in $r_{M1}$, $r_{M2}$ and *q*. The bond lengths and cell parameters are all predicted to approximately 0.5 percent of their values, whereas the chain angles are estimated to within ~5 percent of their values using the regression equations of Table 2.

## Acknowledgments

We are indebted to the Earth Science Section of the National Science Foundation for financial support of this work under grant number DES75-14912. A.R.P., Jr. is supported by an NSF Graduate Fellowship.

## References

Abs-Wurmbach, I. and A. Neuhaus (1976) Das System $NaAlSi_2O_6$ (Jadeit)–$NaCrSi_2O_6$ (Kosmochlor) in Druckbereich von 1 bar bis 25 kb bei 800°C. *Neues Jahrb. Mineral. Abh.*, *127*, 213–241.

Brown, G. E., C. T. Prewitt, J. J. Papike and S. Sueno (1972) A comparison of the structures of low and high pigeonite. *J. Geophys. Res.*, *77*, 5778–5789.

Brown, W. L. (1971) On lithium and sodium trivalent-metal pyroxenes and-crystal-field effects. *Mineral. Mag.*, *38*, 43–48.

Cameron, M., S. Sueno, C. T. Prewitt and J. J. Papike (1973) High-temperature crystal chemistry of acmite, diopside, hedenbergite, jadeite, spodumene, and ureyite. *Am. Mineral.*, *58*, 594–618.

Clark, J. R., D. E. Appleman and J. J. Papike (1968) Bonding in eight ordered clinopyroxenes isostructural with diopside. *Contrib. Mineral. Petrol.*, *20*, 81–85.

———, ——— and ——— (1969) Crystal-chemical characterization of clinopyroxenes based on eight new structure refinements. *Mineral. Soc. Am. Spec. Pap.*, *2*, 31–50.

Dixon, W. J., ed. (1973) *BMD, Biomedical Computer Programs*. University of California Press, Berkeley, 773 p.

Draper N. R. and H. Smith (1966) *Applied Regression Analysis*. John Wiley and Sons, Inc., New York, 407 p.

Drysdale, D. J. (1975) Hydrothermal synthesis of various spodumenes. *Am. Mineral.*, *60*, 105–110.

Finger, L. W. and Y. Ohashi (1976) The thermal expansion of diopside to 800°C, and a refinement of the crystal structure at 700°C. *Am. Mineral.*, *61*, 303–310.

Freed, R. L. and D. R. Peacor (1967) Refinement of the crystal structure of johannsenite. *Am. Mineral.*, *52*, 709–720.

Frondel, C. and C. Klein, Jr. (1965) Ureyite, $NaCrSi_2O_6$, a new meteoritic pyroxene. *Science, 149*, 742–744.

Ghose, S. and C. Wan (1975) Crystal structures of $CaCoSi_2O_6$ and $CaNiSi_2O_6$: crystal chemical relations in *C*2/*c* pyroxenes. *EOS Trans. Am. Geophys. Union*, *56*, 1076.

Hawthorne, F. C. and H. D. Grundy (1973) Refinement of the crystal structure of $NaScSi_2O_6$. *Acta Crystallogr.*, *B29*, 2615–2616.

——— and ——— (1974) Refinement of the crystal structure of $NaInSi_2O_6$. *Acta Crystallogr.*, *B30*, 1882–1884.

——— and ——— (1977) Refinement of the crystal structure of $LiScSi_2O_6$. *Can. Mineral.*, *15*, 50–58.

Higgins, J. B. and P. H. Ribbe (1977) The structure of malayaite, $CaSnOSiO_4$ a tin analog of titanite. *Am. Mineral.*, *62*, 801–806.

Nolan, J. (1969) Physical properties of synthetic and natural pyroxenes in the system diopside–hedenbergite–acmite. *Mineral. Mag.*, *37*, 216–229.

——— and A. D. Edgar (1963) An X-ray investigation of synthetic pyroxenes in the system acmite–diopside–water at 1000 kg/cm$^3$ water-vapour pressure. *Mineral. Mag.*, *33*, 625–634.

Novak, G. A. and G. V. Gibbs (1971) The crystal chemistry of the silicate garnets. *Am. Mineral.*, *56*, 791–825.

Ohashi, Y. and C. W. Burnham (1973) Clinopyroxene lattice deformations: The roles of chemical substitution and temperature. *Am. Mineral.*, *58*, 843–849.

Papike, J. J., C. T. Prewitt, S. Sueno and M. Cameron (1973) Pyroxenes: comparisons of real and ideal structural topologies. *Z. Kristallogr., 138*, 254–273.

Prewitt, C. T., R. D. Shannon and W. B. White (1972) Synthesis of a pyroxene containing trivalent titanium. *Contrib. Mineral. Petrol., 35*, 77–82.

Ribbe, P. H. and A. R. Prunier, Jr. (1976) Stereochemical systematics of eleven *C*2/*c* pyroxenes at room temperature. (abstr.). *Geol. Soc. Am. Abstr. with Programs 8*, 1066–1067.

Rutstein, M. S. and R. A. Yund (1969) Unit-cell parameters of synthetic diopside–hedenbergite solid solutions. *Am. Mineral., 54*, 238–245.

Schlenker, J. L. (1976) *Phenomenological Aspects of Thermal Expansion in Crystals of the Lower Symmetry Classes and the Crystal Structures of* $CaCoSi_2O_6$ *and* $CaNiSi_2O_6$. Ph.D. Dissertation, Virginia Polytechnic Institute and State University, Blacksburg, Virginia.

———, R. K. Popp and F. K. Ross (1977) A refinement of the crystal structures of two synthetic clinopyroxenes: $CaCoSi_2O_6$ and $CaNiSi_2O_6$. *Z. Kristallogr.*, in press.

Shannon, R. D. and C. T. Prewitt (1969) Effective ionic radii in oxides and fluorides. *Acta Crystallogr., B25*, 925–946.

——— and ——— (1970) Revised values of effective ionic radii. *Acta Crystallogr., B26*, 1046–1048.

Smith, J. V., D. A. Stephenson, R. A. Howie and M. H. Hey (1969) Relations between cell dimensions, chemical composition, and site preference of orthopyroxene. *Mineral. Mag., 37*, 90–114.

Smyth, J. R. (1974) The high-temperature crystal chemistry of clinohypersthene. *Am. Mineral., 59*, 1069–1082.

——— and C. W. Burnham (1972) The crystal structures of high and low clinohypersthene. *Earth Planet. Sci. Lett., 14*, 183–189.

Turnock, A. C., D. H. Lindsley and J. E. Grover (1973) Synthesis and unit cell parameters of Ca–Mg–Fe pyroxenes. *Am. Mineral., 58*, 50–59.

Warner, R. D. and W. C. Luth (1974) The diopside–orthoenstatite two-phase region in the system $CaMgSi_2O_6$–$Mg_2Si_2O_6$. *Am. Mineral., 59*, 98–109.

*Manuscript received, November 26, 1976; accepted for publication, February 2, 1977.*